



Biotransformation of multi-walled carbon nanotubes mediated by nanomaterial resistant soil bacteria

Raghuraj S. Chouhan^a, Anjum Qureshi^a, Baris Yagci^b, Mehmet A. Gülgün^c, Volkan Ozguz^a, Javed H. Niazi^{a,*}

^a Sabanci University Nanotechnology Research and Application Center, Orta Mah., 34956 Istanbul, Turkey

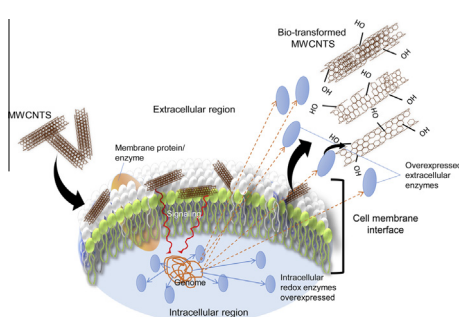
^b Koc University Surface Science and Technology Center (KUYTAM), Rumelifeneri Yolu, 34450 Sariyer, Istanbul, Turkey

^c Faculty of Engineering and Natural Sciences, Sabanci University Orhanli, 34956 Istanbul, Turkey

HIGHLIGHTS

- Isolated nanomaterial-resistant soil bacteria identified as *Trabusiella guamensis*.
- Bacteria bio-transformed multiwalled-carbon nanotubes (MWCNTs) by surface oxidation.
- Bacterial peroxidase lowered its affinity constant (K_m) due to MWCNT-adaptive-drift.
- Eco-friendly, cost-effective and green approach for oxidation of MWCNT is proposed.

GRAPHICAL ABSTRACT



ARTICLE INFO

Article history:

Received 24 February 2016

Received in revised form 3 April 2016

Accepted 4 April 2016

Available online 9 April 2016

Keywords:

Bacteria
Biotransformation
Nanomaterial
Oxidation
Nanotubes

ABSTRACT

In this study, soil bacteria were isolated from nanomaterials (NMs) contaminated goldsmith site and enriched in the presence of multi-walled carbon nanotubes (MWCNTs) in order to obtain resistant bacteria. The isolated resistant bacteria were biochemically and genetically identified as *Trabusiella guamensis*. Redox-enzyme activity and cell viability assay showed molecular adaptation and no membrane damage in resistant bacteria under MWCNTs stress. The resistant bacteria were allowed to interact with engineered MWCNTs in order to study the bio-transformation in their structure. Raman spectra of bio-transformed MWCNTs revealed increased intensity ratio of I_D/I_G with subsequent formation of C=O and COOH groups on the outer walls of nanotubes that were also confirmed by Fourier transform infrared (FTIR) results. X-ray photoelectron spectroscopy (XPS), X-ray diffraction (XRD) and ultraviolet–visible spectroscopy (UV–vis) analysis of bio-transformed MWCNTs revealed surface oxidation of CNTs. The structural changes in concentric walls were also evident from transmission electron microscopy (TEM) images. Our results demonstrated that the biotransformation of MWCNTs was mediated by resistant bacteria through oxidation process. The presented study showed an effective methodology that utilizes NMs resistant microbes for bio-transformation of MWCNTs in different biological settings which will have impact on “green nanotechnology”.

© 2016 Elsevier B.V. All rights reserved.

1. Introduction

Carbon nanotubes (CNTs) gained importance in many applied fields such as composites, conductive materials, sensors, drug delivery vehicles and sorbents [1]. Widespread commercial

* Corresponding author. Tel.: +90 216 483 9879; fax: +90 216 483 9885.

E-mail address: javed@sabanciuniv.edu (J.H. Niazi).

applications and use of CNTs has been linked to their production in large-scale [2]. This may eventually lead to their introduction into the environmental system. In recent years, studies on aggregation and transportation of CNTs have been conducted to understand their possible impact and fate in the environment [3–5]. Most of studies have focused on biocompatibility of CNTs and very few exploring the possibility of their biodegradation [6,7]. A few reports suggest that biocompatibility of CNTs may be attributed to the availability of functional groups on the side walls of nanotubes [8–10]. However, enzymatic catalysis has shown to partially degrade CNTs through biocatalytic oxidations [11–14]. Enzymes that are found to degrade CNTs are horseradish peroxidase (HRP) [11,12,15,16] and neutrophil myeloperoxidase (nMPO) in the presence of H_2O_2 [13].

It is imperative to explore the possibility of CNTs biodegradation mainly by the action of microbes. Recent reports on biodegradation of graphene oxide (GO) by bacteria and the extent to which MWCNTs can be degraded by different bacteria, such as *Burkholderia kururiensis*, *Delftia acidovorans*, and *Stenotrophomonas maltophilia* are given more importance [17,18]. Bacterial community is capable of degrading ^{14}C -labeled MWCNTs into $^{14}CO_2$ in the presence of an external carbon source via co-metabolism. This degradation required external carbon source involving co-metabolism and the cooperation of several microbial consortia [18]. However, structural transformation in MWCNTs during the bacterial degradation process is still unclear. Therefore, degradation or biotransformation of carbon based NMs through different microbial pathways needs to be explored. So far, there are no direct studies reporting on possible biotransformation of CNTs through nanomaterials (NMs) resistant living microorganisms. Natural soil microbial flora requires evolutionary adaptation to the new man-made carbon nanostructures. This can be achieved in the laboratory at a relatively short time if soil bacteria are subjected to selective and forced evolutionary adaptation process.

Here, we report on isolation of soil bacteria from goldsmith contaminated site that are resistant to MWCNTs and identified as *Trabusiella guamensis* which belongs to *Enterobacteriaceae* family and resembles *Salmonella* subgroups. The *T. guamensis* finds niche in a wide variety of environments including marine sediments, various fish species, ocean water and spoiled foods [19,20]. The isolated bacteria were enriched with MWCNTs to induce their strong NMs resistance property. These NM resistant bacteria were further utilized for studying bio-transformation of engineered MWCNTs. Biochemical and physico-chemical methods were employed to identify the pathways and mechanisms for bio-transformation of MWCNTs.

2. Materials and methods

2.1. Materials

MWCNTs used in this study had O.D. \times L 7–15 nm \times 0.5–10 μ m (Arry, Hong Kong). Almar blue, Amplex Red (N-acetyl-3,7-dihydroxyphenoxazine) and Lactate dehydrogenase (LDH) was purchased from Pierce Biotech, Inc. USA. Triton-X 100 was procured from Merck, Germany. Dimethyl Sulfoxide (DMSO) was purchased from Sigma Aldrich, USA. All other reagents used in this study were of analytical grade and filtered through 0.22 μ m sterile filters. Growth studies and enzyme assays were carried out in 96-well NUNC clear microtiter plates (Thermo Scientific, USA). All bacterial studies and related work were carried out under sterile conditions.

2.2. Collection of soil sample and storage

Soil samples were collected from the gold processing industrial wastes from central part of India. The collected soil samples were

appropriately labeled and transported to the laboratory using Standard Operating Procedures (SOPs). The collected soil samples were homogenized in a container constructed of inert material and stored at 4 °C or transferred to appropriate growth medium for the propagation of soil bacteria.

2.3. Isolation and enrichment of NM resistant bacteria

Soil samples (25 g each) were suspended in basal mineral medium (MM) separately, diluted appropriately and filtered through a column with a glass-wool plug to remove undesirable suspended particles from the soil. The basal MM (per liter) contained 3 g KH_2PO_4 , 12.8 g $Na_2HPO_4 \cdot 7H_2O$, 1 g NH_4Cl , 0.5 g NaCl and supplement sources such as $MgSO_4$ (2 mM), $CaCl_2$ (0.1 mM) and glucose (varying from 0.3% to 0.4%). The pH (6.5–7.5) of basal MM and the temperature (25–37 °C) were varied depending upon the growth requirements of the soil microbial flora and modified by removing specific salts accompanied by supplementing with different carbon/nitrogen sources (eg., NH_4NO_3 in place of NH_4Cl). Alternatively, resistant bacteria were also grown in TSB (Tryptic soy broth) medium for rapid screening of mixed bacterial colony characteristics. The TSB medium contained (per liter) 17 g Tryptone (pancreatic digest of casein), 3 g Soytone, 2.5 g dextrose, 5 g Sodium chloride and 2.5 g K_2HPO_4 , pH 7.3. Cultures grown on basal MM were only considered for enrichment while cultures grown in nutrient rich TSB medium were used only for screening colony characteristics because of the possibilities of losing the ability of bacterial adaptation to MWCNTs.

Culture flasks that showed good growth in MM were amended with MWCNTs. MWCNTs suspension was prepared in PBS pH-7.4 containing 0.01% Triton-X 100. The mixture was homogenized using probe ultrasonicator for 15 min. The homogeneous stock suspension of MWCNTs (5–15 μ g/mL) was prepared freshly prior to the start of the experiment. To avoid the undesirable growth of contaminating fungi in cultures, >0.5 μ g/mL of cycloheximide (an anti-fungal agent) was added into the medium before inoculation for three subsequent subcultures and withdrawn when all of the fungi were eliminated. Initially, 5 μ g/mL MWCNTs were amended in the media to interact with the soil bacteria and incubated the flasks at 25–37 °C at 125 rpm and replenished with fresh medium every 30 days interval for over 14 months. Depending upon the resistance of bacteria, MWCNTs concentration was increased to 15 μ g/mL and this concentration was maintained throughout the enrichment process. Thus obtained resistant bacteria were isolated and utilized for characterization.

2.4. Biochemical characteristics of isolated NMs resistant bacteria

In this study, standard biochemical tests that are commonly used (listed in Supporting Information, SI Table S1) for bacterial identification were applied for identification of isolated NM-resistant bacteria. Fresh colonies from all the isolated samples were selected and grown in MM agar containing 0.4% glucose for 48 h. Bacterial colonies from the MM agar plates were picked, suspended in sterile saline solution and vortexed. Each sample was assigned a unique identity to avoid confusion for interpretation of final results. A total of 21 biochemical tests were carried out for the identification of bacteria and the results were interpreted using an online chart (<http://faculty.ivytech.edu/~bsipe/UNKN/ukkey.htm>) according to Bergey's Manual of Systematic Bacteriology [21]. All biochemical tests that were carried out are listed in SI Table S2 using standard commercial biochemical kits (Analytab Products, Inc.).

2.5. Identification of resistant bacteria by genetic method

Genomic DNA from the resistant bacteria was extracted and purified using a Qiagen DNA extraction kit and used as template for amplifying the 27f–1492r regions of the 16S rDNA by PCR using the following universal primer pairs; forward (27f) 5'-AGAGTTG ATCTGGCTCAG-3' and reverse (1492r) 5'-TACCTGTTACGACTT-3'. Each PCR reaction mixture contained 25 μ L of premix Taq (TaqMix, Qiagen), 100 nM of each primer (27f and 1492r), 1 μ L of template DNA (genomic DNA extracted from MWCNT-resistant bacteria), and the total reaction volume finally adjusted to 50 μ L with sterile distilled H₂O. For PCR amplification, following optimized conditions were applied; (i) initial DNA denaturation at 94 °C for 5 min, (ii) 32 cycles of DNA denaturation at 94 °C for 1 min, annealing at 55 °C for 1 min, and amplify at 72 °C for 1 min and (iii) final extension step at 72 °C for 10 min. About 5 μ L of the amplified PCR products thus obtained was resolved on 1% agarose by gel electrophoresis and confirmed the expected PCR product size of 1465 bp. The pure PCR product of 1465 bp size was purified and sequenced. The raw unprocessed sequencing data were directly applied for genetic identification of bacteria by clustering and phylogenetic analysis using BIBI Database (<http://pbil.univ-lyon1.fr/bibi/>). The BIBI tool enabled identifying the type of bacteria based on its 16S rDNA sequences using BLAST and the phylogenetic analysis was performed using ClustalW2 program. The results were analyzed on the basis of sequence composition, information from BLAST and phylogenetic reconstruction on quality of the sequence query and compared the node distances for many sequence clusters from various other related species.

2.6. Interaction of engineered MWCNTs with NMs resistant bacteria and extraction

About 25 mL of resistant bacterial cultures grown for at least 30-days in presence of MWCNTs in MM were separated by centrifugation at 9000 rpm for 10 min. The supernatant was discarded and the pellet containing MWCNTs, cells and cell-debris was washed thrice with pure ethanol and sonicated for 15 min and centrifuged to separate the cells and cell-debris. The supernatant containing cell debris was discarded and the brownish pellet containing MWCNTs was phase separated in a mixture of 1:1 *N*-hexane and deionized water and centrifuged at 9000 rpm for 5 min. A black colored ring of purified MWCNTs appeared at the interface of two solvent phases. Finally, pure MWCNTs were carefully collected in a separate glass vial, washed with deionized water and dried in vacuum desiccators before the sample was used for further characterization.

2.7. Characterizations

SEM images were acquired using a LEO Supra 35VP scanning electron microscope operated at 3 kV. Samples were mounted on a silicon wafer and sputter coated with a thin layer of Pd–Au before taking SEM images. TEM images were acquired using a JEOL JEM-ARM200CFEG UHR equipped with a CCD camera and operated at an acceleration voltage of 100 kV. A drop of the samples was placed directly on a Lacy Carbon Type-A 300 mesh copper grids (Ted Pella, USA), the suspension was drawn through the grid by placing a lint-free tissue under the grid and dried. To reduce the formation of salts on the TEM grid, the grids were briefly washed with a droplet of water and allowed to dry before imaging.

Raman spectra of control (MWCNTs before interaction of resistant bacteria) and test (MWCNTs after interaction of resistant bacteria) MWCNTs samples were measured using Renishaw inVia Reflex Raman Microscope and Spectrometer with spectral resolution of 5 cm^{-1} using a visible excitation at 532 nm laser. Spectral

range was scanned from 110 to 3690 cm^{-1} with a 30 s integration time at a laser power of 10 or 20 mW. MWCNTs were visualized with an integrated Leica microscope allowing confocal measurements with 2.5 μm depth resolution using a 50 \times objective.

Attenuated Total Reflectance-IR (ATR-IR) spectra were used to study functional groups present on MWCNTs transformed structure. Spectra were acquired with a Nicolet iS10 FT-IR Spectrometer (Thermo Scientific, USA) with mercury cadmium telluride detector (4 cm^{-1} resolution) equipped with a diamond crystal in single reflection mode. Ultraviolet–visible (UV–vis) spectra were obtained using NanoDrop 2000 spectrophotometer (Thermo Scientific NanoDrop Products).

X-ray diffraction analyses were carried out using X-ray diffractometer (Bruker D8 DISCOVER, Bruker AXS GmbH, Karlsruhe, Germany). The high resolution XRD patterns of samples were measured at 3 Kw with Cu target using scintillation counter ($\lambda = 1.5406 \text{ \AA}$) at 40 kV in the range of $2\theta = 2\text{--}90^\circ$. The dried extracted sample of MWCNTs (control and test) was placed on glass slide followed by a drop of ethanol and allowed to dry and placed on the sample holder for XRD analysis. The control and test MWCNTs were mounted on a carbon tape and XPS spectra were recorded using a Thermo Scientific K-Alpha X-ray photoelectron spectrometer. Monochromatized Al K_{α} radiation (Al $K_{\alpha} = 146.3 \text{ eV}$) was used as the X-ray source and flood gun was used for charge compensation during the measurements. The X-ray spot size was approximately 400 μm . Electron take-off angle between the sample surface and the axis of the analyzer lens was set to 90°. Spectra were recorded using Avantage 5.9 data system. The binding energy scale was calibrated by assigning the C1s signal at 284.5 eV.

2.8. Redox-enzyme activity of resistant bacteria with and without engineered MWCNTs

Preparation of cell-free extracts of resistant bacteria for redox-enzyme activity assay is given in SI section

2.9. Resistant bacterial growth studies with and without engineered MWCNTs

The isolated resistant bacteria were allowed to grow in MM containing 0.4% glucose as the only carbon and energy source in a 96-well clear microtiter plate. 150 μL of MM with (test) or without (control) MWCNTs were mixed with 25 μL bacterial cells and the starting A_{600} was adjusted to 0.13. Homogenous suspension of control and extracted bio-transformed MWCNTs in PBS containing 0.01% Triton-X 100 was added to each well to give final concentrations of 15 $\mu\text{g/mL}$ MWCNTs in 200 $\mu\text{L/well}$. The plate was then incubated at 37 °C in a Synergy™ HTX microplate reader (Bio-Tek) with continuous shaking mode and the A_{600} was recorded every 5 min for 48 h.

3. Results and discussions

3.1. Isolation and enrichment of NM resistant bacteria

In this study, soil samples near the goldsmith industrial waste disposal sites were collected that had a prior history of NM contamination as a source of persistent bacteria, capable of utilizing MWCNTs (Fig. 1). This allowed exploring potential nano-size-stress-resistance in soil bacterial population, because it is reported that soil sample from gold processing industries has been found to contain gold leachates with nano/micro particles or colloidal suspensions [22,23]. Metallic gold was detected in the form of micro precipitates on the biomass surfaces as well as in colloidal form as nano-particles in the solution. A number of other studies

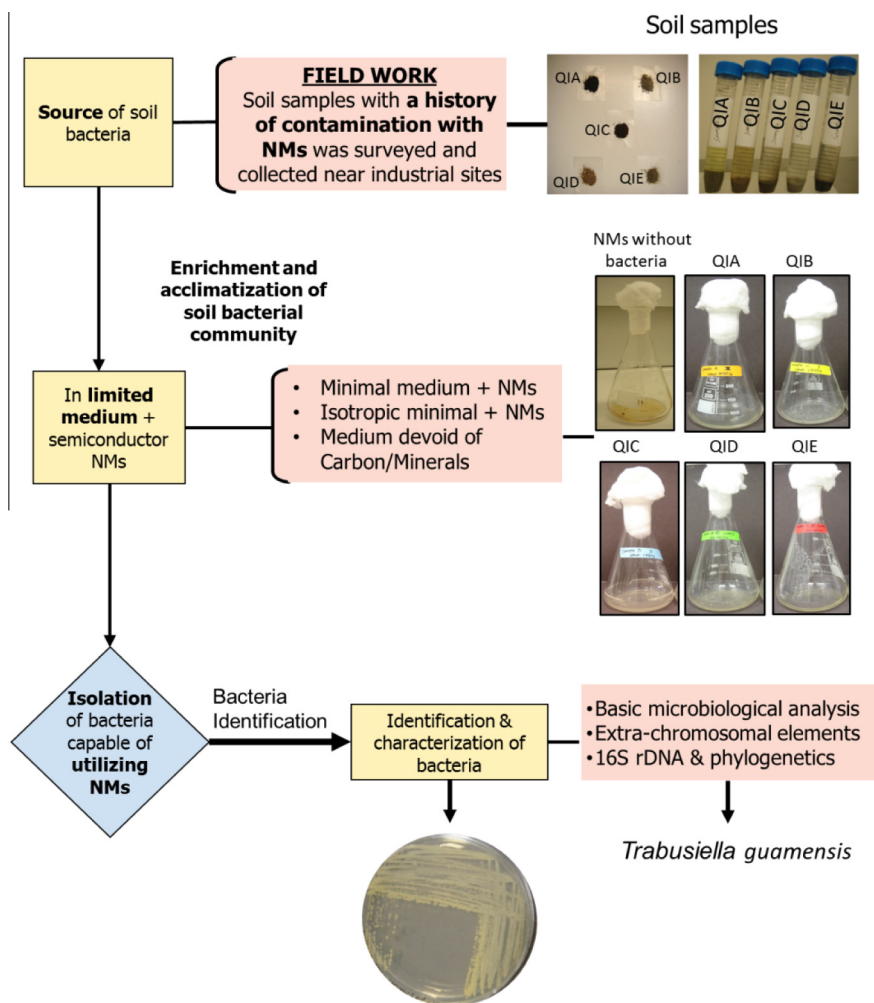


Fig. 1. Schematic representation of isolation and identification of NMs resistant bacteria from field to lab.

showing the presence of nanoparticles in gold scrap (waste) have been reported [24]. Therefore, NMs contaminated soil bacteria could acquire greater adaptation which would further lead to bio-transformation of NMs through oxidation or reduction processes. Here, the soil bacteria isolated from NMs contaminated soil samples (QIA, QIB, QIC, QID and QIE) were incubated with MWCNTs for adaptation and obtained resistant bacteria (Fig. S1). Each soil sample was suspended in the MM and divided into two pools for control and test flasks, respectively and screened for the influence of growth in presence of CNTs. Images of flasks that showed positive growth in presence of MWCNTs were documented for comparison with respective controls. The enriched soil microbial population was subjected to acclimatization (adaptation) to efficiently grow and resist against MWCNTs under artificial environment, alternatively in a climate chamber (Fig. 1).

The turbidity in test flasks is the indicative of the positive growth of bacteria in MWCNTs supplemented media. The resistant bacteria on MM-agar plates were obtained after 14-months of enrichment process in the artificially created environment by following similar conditions (mineral media, salt concentrations, pH and temperature) and identified at species level.

The resistant mixed bacterial population was subjected to screening and isolation of the most dominant bacterial candidate and examined using SEM (Fig. 2a). This bacterial candidate showed adaptation with a high degree of survival and tolerance to MWCNTs. SEM image of isolated resistant bacteria interacted with

MWCNTs (Fig. 2b–d). MWCNTs formed tightly wrapped bundles over and around the cells (Fig. 2c). Closer examination of an individual cell from the cells–CNT aggregates revealed tight coiling of MWCNTs around the outer cell-surface (inset Fig. 2d). The close proximity of MWCNTs at the cell-interface enables interaction between MWCNTs and extracellular oxidative enzymes secreted by the viable cells. Therefore, viability of resistant bacteria with or without MWCNTs interactions were compared to determine any reduction in colony forming units (CFU). Our results revealed that the cell morphology tend to remain intact and the cells proliferated at a normal metabolic rate before and after their interaction with MWCNTs (Fig. 2a–d and insets).

3.2. Identification of resistant bacteria by biochemical and genetic methods

The biochemical tests enabled identifying different bacterial species as a result of various metabolic properties of bacterial cells. The results of biochemical tests to identify the NM-resistant bacteria were scored as “+” or “–” codes through color change or release of gases according to the standard protocol for each sample (Table S1) [21]. Based on the biochemical characteristics, the NM-resistant bacteria were identified as aerobic (catalase positive) and exhibited negative carbohydrate fermentation tests indicating non-fermenting nature of bacteria (Tables S1 and S2). These test results in combination with others including Gram staining

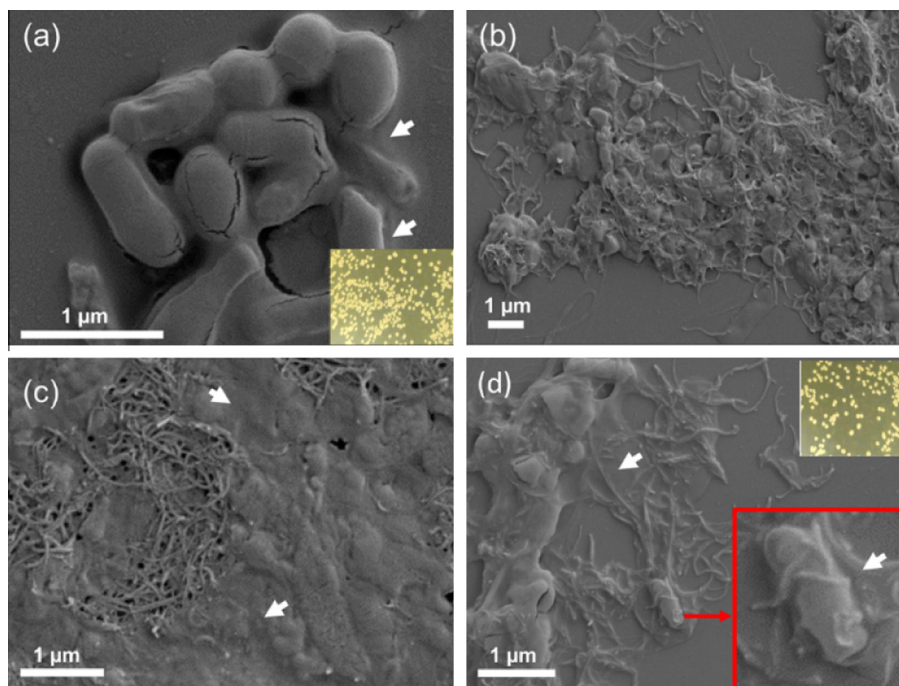


Fig. 2. SEM images of resistant bacteria and MWCNTs aggregates; (a) isolated resistant bacteria; (b and c) resistant bacteria and MWCNT-bundles forming a thick blanket-like structure. (d) A resistant bacterial cell dispersed from the MWCNT-aggregates showing strong wrapping by MWCNTs. The inset image at the right-bottom in figure (d) shows an enlarged image of an intact bacterium wrapped by MWCNTs. Culture plates showing viable cell colonies of resistant bacteria are shown as insets in figures (a and d).

enabled identifying as Gram negative bacteria which was rod shaped in structure (Fig. S1). The enriched bacterium was subjected to genetic identification using 16S rRNA sequencing followed by phylogenetic analysis (Fig. S2). The results showed that the resistant bacteria was *T. guamensis* which is mainly found in dusts or soil [25].

3.3. Redox-enzyme activity and viability test of resistant bacteria

The adaptation and viability of resistant bacteria were studied by measuring LDH enzyme activity assay, cell growth, and viability assay with Almar blue. Redox enzyme activities from resistant bacterial cells were measured before and after their interaction with MWCNTs (Fig. 3). The peroxidase enzyme activity from cell-free extracts of resistant bacteria in presence of MWCNTs increased by ~50% (specific activities = 3.5 $\mu\text{moles}/\text{min}/\text{mg}$ protein) as compared with enzyme activities in cells grown without MWCNTs (2.5 $\mu\text{moles}/\text{min}/\text{mg}$ protein). The enzyme reaction was analyzed in terms of Michaelis–Menten constant (K_m) which is the measure of the substrate's affinity towards the peroxidase enzyme in cell-free extracts of resistant bacteria. The K_m value of peroxidase resis-

tant bacteria after interaction with MWCNTs was higher with H_2O_2 and AR ($K_m = 63$ and $102 \mu\text{M}$) as compared with cells grown without MWCNTs ($K_m = 35$ and $48 \mu\text{M}$, respectively). The enzymatic reaction rate was rapid with low K_m value for peroxidase from the resistant bacteria before interaction with MWCNTs (Fig. 3a and b). In contrary, higher K_m value with delayed V_{max} was observed with peroxidase of resistant bacteria after they interacted with MWCNTs (Fig. 3a and b). This delayed response and high K_m of peroxidase of resistant bacteria suggested conformational changes in the active site of enzyme in resistant bacteria. It is reported that increase in the catalytic activity of bacteria with high K_m value is linked to adaptive drift and substrate binding specificity [26,27]. Our results showed that the peroxidase of resistant bacteria with high K_m value in presence of MWCNTs suggests molecular adaptation of bacteria against the MWCNTs stress. This may have allowed resistant bacteria to remain viable for longer period of time and facilitate bio-transformation of NMs.

Growth rates of resistant bacteria with (test) and without (control) MWCNTs are shown in Fig. 3c. It was observed that the growth rate of resistant bacteria tends to moderately decline over time in presence of MWCNTs due to slower metabolic activity as

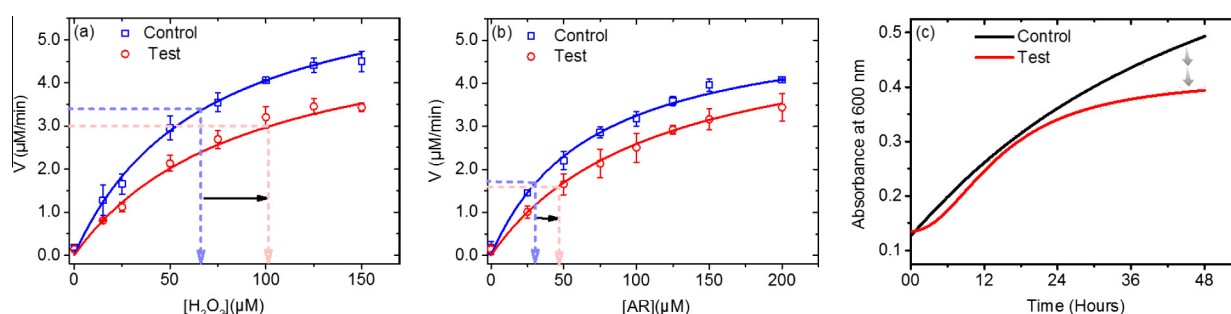


Fig. 3. Effect of bi-substrate concentrations of (a) $[\text{H}_2\text{O}_2]$ and (b) $[\text{AR}]$ on the rate of total intracellular peroxidases (250 μg protein) extracted from resistant bacterial samples grown without MWCNTs (control) and with MWCNTs (test), and (c) time dependent growth studies of control and test resistant bacteria.

compared with control (Fig. 3b). The higher K_m values of cellular peroxidase in resistant bacteria can be attributed to the slower metabolic rate that affected the growth of resistant bacteria with MWCNTs. The above result indicated that the adaptation of resistant bacteria to engineered MWCNTs was due to changes in cellular enzyme activity. It is documented that intracellular enzymes adapted to cellular stress seemed to enhance both K_m and K_{cat} for other enzymes, such as xylanase isolated from the Antarctic bacterium *Pseudoalteromonas haloplanktis* [28]. Our findings suggested that similar adaptation of engineered MWCNTs stress was acquired by NMs resistant bacteria [28]. The bacterial enzymes may exhibit a higher K_m value to acquire a lower affinity for the substrates which is essential for cellular viability under stress. Therefore, we also confirmed cellular viability (% mortality) of resistant bacteria with varying concentrations of MWCNTs by standard LDH and Almar blue viability assays. Both assays showed no significant membrane damage in resistant bacteria against the MWCNTs indicating their positive adaptation to MWCNTs stress (Fig. S3).

3.4. Characterizations

3.4.1. FTIR and Raman results

MWCNTs interacted with resistant bacteria (test) and control MWCNTs (without their interaction with resistant bacteria) were extracted from the media and analyzed by FTIR and Raman spectroscopy (Fig. 4a and b). Fig. 4a shows FTIR spectra of bio-transformed MWCNT sample (test) that showed a peak at 1730 cm^{-1} which corresponds to the stretching vibration of C=O from the carboxylic groups (COOH) [29]. Peaks at 1375 and 1283 cm^{-1} corresponded to the $\delta(\text{O-H})$ and $\nu(\text{C-O})$ bonds, respectively that are associated with carboxylic groups [30]. Peak at 1651 cm^{-1} can be attributed to C=C stretch vibrations while 1531 cm^{-1} peak was assigned to aromatic ring stretching coupled to in-plane deformation of MWCNTs [31]. The structural variations in the outer tubular bundles in test sample were well distinguished from the respective control sample (Fig. 4a). This result indicated the changes in atomic structure of MWCNTs occurred due to the bio-catalytic action of bacteria adhered on the walls of CNTs (Fig. 4a).

Raman spectra of test sample showed three characteristic peaks that represented D, G, and G' , respectively, as expected for a typical MWCNTs structure (Fig. 4b). However, the I_D/I_G intensity ratio with test and control MWCNTs significantly varied, where I_D/I_G ratio for MWCNTs increased from 0.7 to 1.2 in test/bio-transformed MWCNTs. Similar increase in the intensity ratio (I_D/I_G) of the D-band to G-band for MWCNTs and other carbon nanostructures has been used as evidence for oxidation or side-wall functionalization and conversion of sp^2 hybridized carbon atoms in the MWCNTs to sp^3 hybridization [32,33]. Therefore, a significant

increase in the I_D/I_G ratio of test MWCNTs in this study can be attributed to oxidation or side-wall functionalization of MWCNTs caused by the bacterial catalysis. It also implied that *T. guamensis* bacteria created more transformed attributes on the nanotubes on their external surfaces. Raman and FTIR spectra of MWCNTs test samples clearly indicated that the nanotubes were structurally degraded through possible surface oxidation. Increased D band intensity can be attributed to the structural modification due to the formation of different functional groups on the outer surface of nanotubes (Fig. 4b).

3.4.2. XRD and UV-visible spectroscopy

The XRD patterns and UV-visible spectra of control and test MWCNTs are shown in Fig. 5a and b. The X-ray diffraction patterns of control MWCNTs showed a diffraction peak for graphitic nanosheets at $2\theta = 25.27^\circ$ corresponding to the in plane stretching (Fig. 5a). A new peak was emerged at 8.81° ($d = 10\text{ \AA}$; test) in XRD pattern of test MWCNTs which corresponded to the C=O group. These changes revealed formation of new functional groups mediated by resistant bacteria [34]. It was also observed that the C-axis spacing increased from 3.6 to 3.7 \AA in test MWCNTs that is possible due to the creation of abundant oxygen-containing functional groups on the surfaces of MWCNTs (Fig. 5a).

UV-visible spectra of control and test MWCNTs exhibited characteristic peaks at 240 nm (corresponding to $\pi-\pi^*$ transitions of C=C bonds) due to π electrons of the double bonds in the MWCNTs (Fig. 5b). After resistant bacteria interaction with test MWCNTs, a new shoulder peak was seen at 302 nm (due to $n-\pi^*$ transitions of COOH groups) indicating a transition occurred due to an unshared pair of electrons of the $-\text{C}=\text{O}$ bond in the $(-\text{COO})$ carbonyl group [35,36].

3.4.3. X-ray photoelectron spectroscopy

The changes in oxidation level of MWCNTs in test (MWCNTs after interaction with resistant bacteria) and control (MWCNTs without bacterial interaction) samples were analyzed by recording XPS spectra (Fig. 6a–c). The C1s spectrum of test samples resolved into different characteristic peaks (Fig. 6b). The peaks centered at binding energies of 284.5 eV , 286.3 eV and 289.2 eV were attributed to C–C, C–O and O=C–O respectively in control and test MWCNTs sample [37]. The intensities of peaks corresponding to C–O and O=C–O relatively increased in test MWCNTs compared with control MWCNTs (Fig. 6a and b).

The survey spectra of test MWCNTs showed intense O1s peaks indicating the presence of oxygen species on the nanotubes. The relative percentage of oxygen containing carbon species on the surface of test MWCNTs was increased from $\sim 6\%$ to $\sim 13\%$ (Fig. 6c, Table 1) which revealed the surface oxidation of CNTs. These results were well supported with the XRD and UV spectral

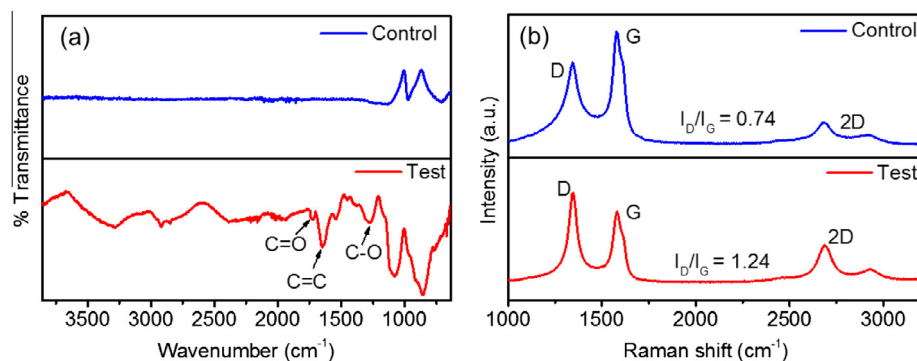


Fig. 4. (a) FTIR and (b) Raman spectra of control and test MWCNTs samples.

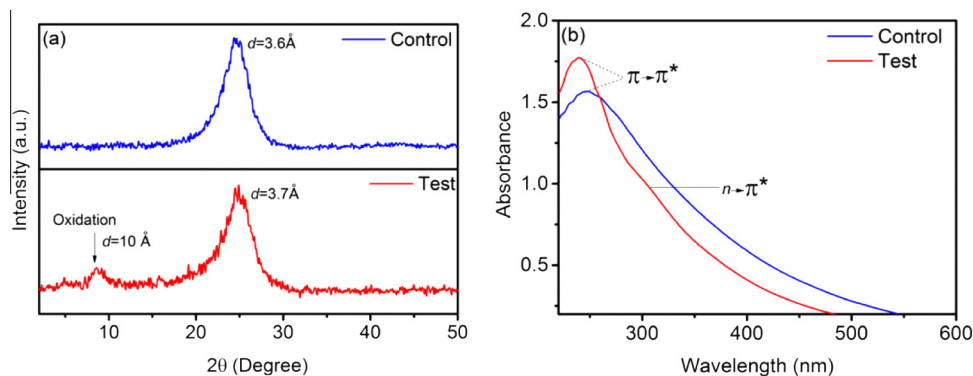


Fig. 5. (a) XRD and (b) UV-vis spectra of control and test MWCNTs samples.

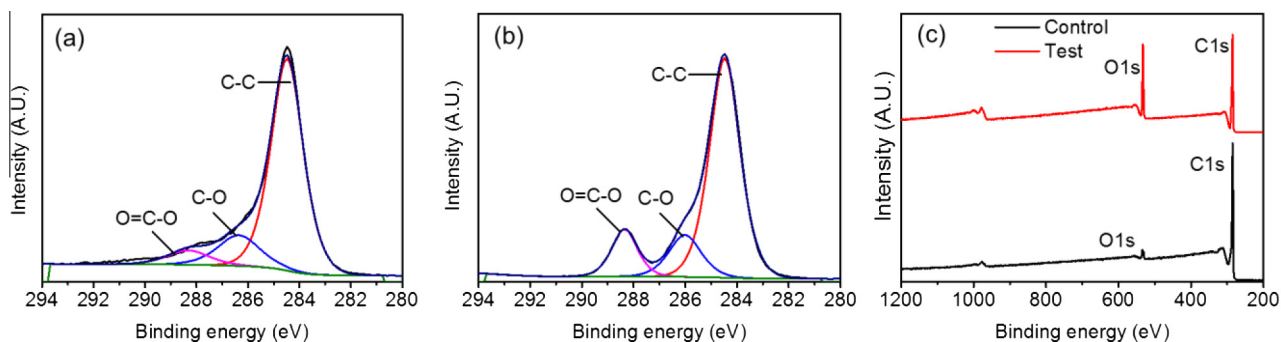


Fig. 6. XPS C1s spectra of (a) control, (b) test MWCNTs and (c) survey spectra of control and test MWCNTs.

analysis that showed emergence of a new peak at 8.81° in XRD and $n-\pi^*$ transitions of COOH groups in UV spectra (Fig. 6a and b). These results are consistent with a previous report, where chemical oxidation of CNTs by strong chemical oxidants also showed similar oxygen containing functional groups on the surfaces [38].

3.4.4. TEM analysis

The changes occurred on the concentric walls of test MWCNTs were observed by high resolution (HR) TEM image examination. The HR-TEM images as well as histograms for control and test MWCNTs samples were shown in Fig. 7a–j. TEM images of test MWCNTs showed changes in the outermost sidewalls of CNTs (Fig. 7f–i). Number of concentric walls in test MWCNTs tended to progressively reduce and started to disappear upon interaction with resistant bacteria as compared to control sample (Fig. 7f–j). The TEM surface profiles of test MWCNTs structure showed decrease in the number of CNT-walls by $\sim 25\%$ relative to control MWCNTs due to their interaction with resistant bacteria (Fig. 7a–f). The outermost walls of control CNTs were found to be long and straight with defect-free sidewall structures (Fig. 7a–d). After their interaction with resistant bacteria, the overall struc-

tures of CNTs undergo roughening on the surface of sidewalls. The roughness generated on the surface of test MWCNTs was probably due to bacterial bio-catalytic oxidation or exfoliation of a few layers of MWCNTs (Fig. 7f–j). Resistant bacteria also induced distortions in the linearity of the test MWCNTs structure due to mutilation as observed in TEM images (Fig. 7f). The convoluted, distorted bundles and thinning of walls in CNTs structure upon interaction with bacteria has been previously reported [15]. Such observations in atomic structure of CNTs supported the fact that outer sidewalls of nanotubes are more accessible or vulnerable to bacteria, and thus caused degradation of outer CNT layers.

The underlying mechanism of bacterial bio-transformation of MWCNTs can be explained by the following. First, the bacteria are able to resist to MWCNTs as evidenced by their growth and survival in presence of MWCNTs (Fig. S3). The resistance of bacteria to MWCNTs is due to intracellular adaptations to MWCNT-stress, which was confirmed by the changes in total cellular peroxidases relative to control as a measure for adaptation to stress (Figs. 3a–c; S3). Bacteria tend to interact with external perturbations such as in this case, MWCNTs that induce a series of cellular changes to mitigate the stress. One such possible mitigation is overexpression of stress-related enzymes, such as intracellular or extracellular redox enzymes and peroxidases. We here measured the total cellular redox status using peroxidase activity, which provided clues to cellular adaptation events against MWCNTs (Fig. 3a and b). Following this, structural changes that occur on MWCNTs provided evidence to bacterial interaction and recruitment of bacterial redox enzymes (peroxidases) for subsequent detoxification. All these changes were probed through identifying structural changes in MWCNTs with appropriate controls. The roughness at the outermost layer on the test/bio-transformed MWCNTs seen in TEM images is a clear evidence of surface oxidation, induced by their interaction at the interface of outer bacterial

Table 1

Atomic percentages of C–O in XPS spectra of control and test/bio-transformed MWCNT samples.

Functional groups	XPS spectral features					
	Control MWCNTs			Test/bio-transformed MWCNTs		
	Peak	FWHM	At (%)	Peak	FWHM	At (%)
C–C	284.48	1.47	67	284.47	1.38	55.6
C–O	286.36	1.92	11.71	286.01	1.46	19.26
O=C–O	288.32	1.92	5.93	288.35	1.16	13.07

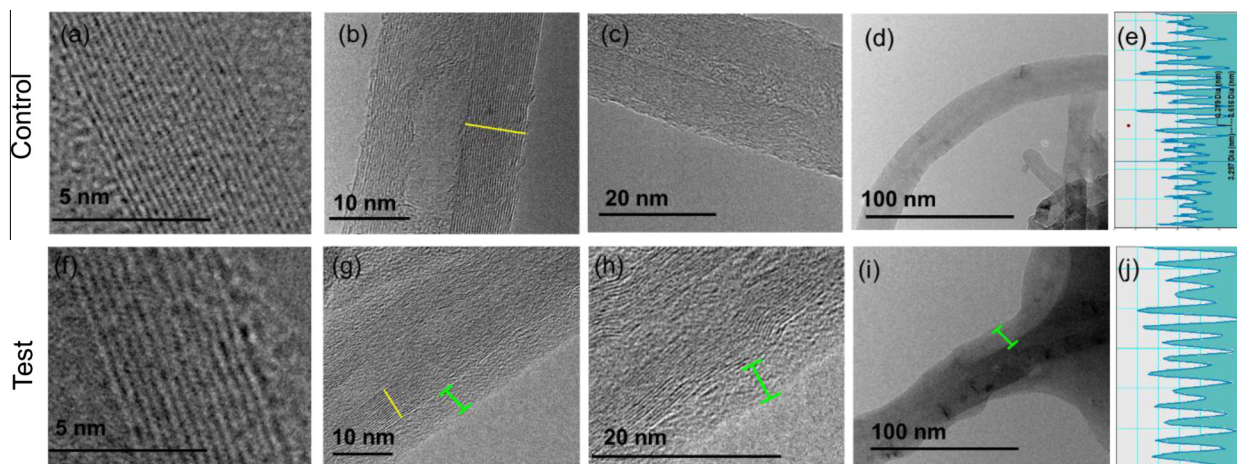


Fig. 7. High resolution TEM images of MWCNTs at different magnifications. (a–d) Images of control MWCNTs showing smooth nanotube surface. (e) Histogram of control MWCNTs generated from the TEM image. (f–i) Bio-transformed (test) MWCNTs showing reduced concentric walls and rough nanotube surface due to the resistant bacterial oxidation (highlighted with green lines). (j) Histogram of test MWCNTs generated from TEM images. The reduced number of nanotube walls were compared from histograms (e and j) representing the outermost walls as spikes present in control and bio-transformed MWCNTs. The reduced number of walls in test was due to the resistant bacterial oxidation as compared with control.

membrane (Fig. 2d). Changes in structural attributes of bio-transformed MWCNTs as observed in TEM images can be attributed to the removal of amorphous carbon while bio-catalytically oxidizing MWCNT sidewalls (Figs. 3a–b; 7f–i). Results of a combination of physico-chemical characterizations of bio-transformed MWCNTs revealed that the oxidation was due to the presence of biologically introduced C=O and/or COOH groups (Figs. 4a–b, 5a and b, 6a–c and 7f–i). The above results provided unambiguous structural information on the effect of biological oxidation in MWCNTs.

4. Conclusions

In this study, we presented a green approach in which NMs contaminated soil resistant bacteria were utilized for bio-transformation of MWCNTs. The isolated and enriched NMs resistant bacteria were biochemically and genetically identified as *T. guamensis*. Redox-enzyme activity and cell viability test showed the molecular adaptation of isolated bacteria during enrichment process under MWCNTs exposure. Further, the resistant bacteria showed biotransformation/surface oxidation of MWCNTs through formation of C=O and COOH groups on the outer walls of nanotubes and increased in oxygen species on surface of the CNTs. The structural changes such as roughness, distortion and reduced number of concentric walls of MWCNTs upon interaction with NM resistant bacteria were also observed. Our results demonstrated that the bio-transformations of MWCNTs were induced through oxidation and partial catalytic degradation processes which were mediated by NMs resistant bacteria. The proposed approach has a potential to use resistant bacteria for bio-transformation of MWCNTs with new properties that are safe for industrial applications.

Acknowledgements

This work was supported by the Scientific and Technological Research Council of Turkey (TUBITAK) with Project Grant No. 112Y309 to JHN.

Appendix A. Supplementary data

Supplementary data associated with this article can be found, in the online version, at <http://dx.doi.org/10.1016/j.cej.2016.04.019>.

References

- [1] V. Popov, Carbon nanotubes: properties and application, *Mat. Sci. Eng. R* 43 (2004) 61–102.
- [2] M.F.L. De Volder, S.H. Tawfik, R.H. Baughman, A.J. Hart, Carbon nanotubes: present and future commercial applications, *Science* 339 (2013) 535–539.
- [3] K.L. Chen, B.A. Smith, W.P. Ball, D.H. Fairbrother, Assessing the colloidal properties of engineered nanoparticles in water: case studies from fullerene C 60 nanoparticles and carbon nanotubes, *Environ. Chem.* 7 (2010) 10.
- [4] A.J. Kennedy, M.S. Hull, J.A. Steevens, K.M. Dontsova, M.A. Chappell, J.C. Gunter, C.A. Weiss, Factors influencing the partitioning and toxicity of nanotubes in the aquatic environment, *Environ. Toxicol. Chem.* 27 (2008) 1932.
- [5] E.J. Petersen, L. Zhang, N.T. Mattison, D.M. O'Carroll, A.J. Whelton, N. Uddin, T. Nguyen, Q. Huang, T.B. Henry, R.D. Holbrook, K.L. Chen, Potential release pathways, environmental fate, and ecological risks of carbon nanotubes, *Environ. Sci. Technol.* 45 (2011) 9837–9856.
- [6] L. Lacerda, M.A. Herrero, K. Venner, A. Bianco, M. Prato, K. Kostarelos, Carbon-nanotube shape and individualization critical for renal excretion, *Small* 4 (2008) 1130–1132.
- [7] A. Ruggiero, C.H. Villa, E. Bander, D.A. Rey, M. Bergkvist, C.A. Batt, K. Manova-Todorova, W.M. Deen, D.A. Scheinberg, M.R. McDevitt, Paradoxical glomerular filtration of carbon nanotubes, *Proc. Natl. Acad. Sci.* 107 (2010) 12369–12374.
- [8] M.L. Schipper, N. Nakayama-Ratchford, C.R. Davis, N.W.S. Kam, P. Chu, Z. Liu, X. Sun, H. Dai, S.S. Gambhir, A pilot toxicology study of single-walled carbon nanotubes in a small sample of mice, *Nat. Nanotechnol.* 3 (2008) 216–221.
- [9] C.M. Sayes, F. Liang, J.L. Hudson, J. Mendez, W. Guo, J.M. Beach, V.C. Moore, C.D. Doyle, J.L. West, W.E. Billups, K.D. Ausman, V.L. Colvin, Functionalization density dependence of single-walled carbon nanotubes cytotoxicity in vitro, *Toxicol. Lett.* 161 (2006) 135–142.
- [10] L. Lacerda, H. Ali-Boucetta, M.A. Herrero, G. Pastorin, A. Bianco, M. Prato, K. Kostarelos, Tissue histology and physiology following intravenous administration of different types of functionalized multiwalled carbon nanotubes, *Nanomedicine* 3 (2008) 149–161.
- [11] B.L. Allen, P.D. Kichambare, P. Gou, I.I. Vlasova, A.A. Kapralov, N. Konduru, V.E. Kagan, A. Star, Biodegradation of single-walled carbon nanotubes through enzymatic catalysis, *Nano Lett.* 8 (2008) 3899–3903.
- [12] B.L. Allen, G.P. Kotchey, Y. Chen, N.V.K. Yanamala, J. Klein-Seetharaman, V.E. Kagan, A. Star, Mechanistic investigations of horseradish peroxidase-catalyzed degradation of single-walled carbon nanotubes, *J. Am. Chem. Soc.* 131 (2009) 17194–17205.
- [13] V.E. Kagan, N.V. Konduru, W. Feng, B.L. Allen, J. Conroy, Y. Volkov, I.I. Vlasova, N.A. Belikova, N. Yanamala, A. Kapralov, Y.Y. Tyurina, J. Shi, E.R. Kisin, A.R. Murray, J. Franks, D. Stolz, P. Gou, J. Klein-Seetharaman, B. Fadeel, A. Star, A.A. Shvedova, Carbon nanotubes degraded by neutrophil myeloperoxidase induce less pulmonary inflammation, *Nat. Nanotechnol.* 5 (2010) 354–359.
- [14] X. Liu, R.H. Hurt, A.B. Kane, Biodurability of single-walled carbon nanotubes depends on surface functionalization, *Carbon* 48 (2010) 1961–1969.
- [15] J. Russier, C. Ménard-Moyon, E. Venturelli, E. Gravel, G. Marcolongo, M. Meneghetti, E. Doris, A. Bianco, Oxidative biodegradation of single- and multi-walled carbon nanotubes, *Nanoscale* 3 (2011) 893–896.
- [16] Y. Zhao, B.L. Allen, A. Star, Enzymatic degradation of multiwalled carbon nanotubes, *J. Phys. Chem. A* 115 (2011) 9536–9544.
- [17] E.C. Salas, Z. Sun, A. Lüttge, J.M. Tour, Reduction of graphene oxide via bacterial respiration, *ACS Nano* 4 (2010) 4852–4856.
- [18] L. Zhang, E.J. Petersen, M.Y. Habteselassie, L. Mao, Q. Huang, Degradation of multiwall carbon nanotubes by bacteria, *Environ. Poll.* 181 (2013) 335–339.

- [19] H. Reichenbach, *Byssovorax cruenta* gen. nov., sp. nov., nom. rev., a cellulose-degrading myxobacterium: rediscovery of 'Myxococcus cruentus' Thaxter 1897, *Int. J. Syst. Evol. Microbiol.* 56 (2006) 2357–2363.
- [20] E. Rurangwa, D. Sipkema, J. Kals, M. ter Veld, M. Forlenza, G.M. Bacanu, H. Smidt, A.P. Palstra, Impact of a novel protein meal on the gastrointestinal microbiota and the host transcriptome of larval zebrafish *Danio rerio*, *Front. Physiol.* 6 (2015).
- [21] N.R. Krieg, Bacterial classification – an overview, *Can. J. Microbiol.* 34 (1988) 536–540.
- [22] M.L. Saccà, C. Fajardo, M. Martínez-Gomariz, G. Costa, M. Nande, M. Martin, Molecular stress responses to nano-sized zero-valent iron (nZVI) particles in the soil bacterium *Pseudomonas stutzeri*, *PLoS ONE* 9 (2014) e89677.
- [23] A. Manni, G. Saviano, P. Massacci, Characterization of gold particles in recoverable waste matrix, *Min. Eng.* 14 (2001) 1679–1684.
- [24] S. Syed, Recovery of gold from secondary sources—a review, *Hydrometallurgy* 115–116 (2012) 30–51.
- [25] L.S. McClung, *Bergey's Manual of Systematic Bacteriology, Volume 1.*: Edited by Noel R. Krieg. The Williams & Wilkins Co., Baltimore, 1984, 964 pp. \$80.00, *Int. J. Sys. Evol. Bacteriol.* 35 (1985) 408–408.
- [26] M. Bentahir, G. Feller, M. Aittaleb, J. Lamotte-Brasseur, T. Himri, J.P. Chessa, C. Gerday, Structural, kinetic, and calorimetric characterization of the cold-active phosphoglycerate kinase from the Antarctic *Pseudomonas* sp. TAC118, *J. Biol. Chem.* 275 (2000) 11147–11153.
- [27] S. D'Amico, T. Collins, J.-C. Marx, G. Feller, C. Gerday, Psychrophilic microorganisms: challenges for life, *EMBO Rep.* 7 (2006) 385–389.
- [28] T. Collins, M.A. Meuwis, I. Stals, M. Claeysens, G. Feller, C. Gerday, A novel family 8 xylanase, functional and physicochemical characterization, *J. Biol. Chem.* 277 (2002) 35133–35139.
- [29] W. Sun, Z. Huang, L. Zhang, J. Zhu, Luminescence from multi-walled carbon nanotubes and the Eu(III)/multi-walled carbon nanotube composite, *Carbon* 41 (2003) 1685–1687.
- [30] C. Velasco-Santos, A.L. Martínez-Hernández, V.M. Castaño, Hydrogen bonding of polystyrene latex nanospheres to sidewall carbon nanotubes, *J. Phys. Chem. B.* 108 (2004) 18866–18869.
- [31] X. Chen, X. Chen, M. Lin, W. Zhong, X. Chen, Z. Chen, Functionalized multi-walled carbon nanotubes prepared by in situ polycondensation of polyurethane, *Macromol. Chem. Phys.* 208 (2007) 964–972.
- [32] P. Khanra, T. Kuila, N.H. Kim, S.H. Bae, D.S. Yu, J.H. Lee, Simultaneous bio-functionalization and reduction of graphene oxide by baker's yeast, *Chem. Eng. J.* 183 (2012) 526–533.
- [33] S. Lee, J.W. Peng, C.H. Liu, Raman study of carbon nanotube purification using atmospheric pressure plasma, *Carbon* 46 (2008) 2124–2132.
- [34] A.S.K. Kumar, S.J. Jiang, W.L. Tseng, Effective adsorption of chromium(VI)/Cr(III) from aqueous solution using ionic liquid functionalized multiwalled carbon nanotubes as a super sorbent, *J. Mater. Chem. A* 3 (2015) 7044–7057.
- [35] A.B. Dichiaro, T.J. Sherwood, J. Benton-Smith, J.C. Wilson, S.J. Weinstein, R.E. Rogers, Free-standing carbon nanotube/graphene hybrid papers as next generation adsorbents, *Nanoscale* 6 (2014) 6322–6327.
- [36] H. Hu, B. Zhao, M.A. Hamon, K. Kamaras, M.E. Itkis, R.C. Haddon, Sidewall functionalization of single-walled carbon nanotubes by addition of dichlorocarbene, *J. Am. Chem. Soc.* 125 (2003) 14893–14900.
- [37] F. Jia, L. Wu, J. Meng, M. Yang, H. Kong, T. Liu, H. Xu, Preparation, characterization and fluorescent imaging of multi-walled carbon nanotube-porphyrin conjugate, *J. Mater. Chem.* 19 (2009) 8950.
- [38] K.A. Wepasnick, B.A. Smith, K.E. Schrote, H.K. Wilson, S.R. Diegelmann, D.H. Fairbrother, Surface and structural characterization of multi-walled carbon nanotubes following different oxidative treatments, *Carbon* 49 (2011) 24–36.